Article

# Electric Field and Ion Diffusion Triggered Precisely Regulated Construction of Micron-scale Water-based Polymer Films: a Detailed Mechanistic Exploration

WANG Dan[1,2,3], LIU Jinfang[2,3], YANG Shuqi[2,3], JI Xin[2,3], WANG Yuliang[2,3], OMONIYI Ahmed Olalekan[1,2,3], ZHANG Jianfu[2,3]✉ and SU Zhongmin[1,2,3]✉

Received December 23, 2021
Accepted January 23, 2022


Water-based polymer films can be readily deposited onto a wide range of metallic materials as an environmentally friendly coating through the demulsification-induced fast solidification(DIFS) method. However, there is still a lack of in-depth understanding of the demulsification process of the water-based emulsions and their deposition processes. Herein, we demonstrate that the build-up process of the commercial water-based micron-scale waterborne polyurethane, polyvinyl acetate, polyurethane acrylate, and natural rubber polymer films is affected by the collective effect of electric field and ion diffusion exerted by anode-cathode electrode pairs, applied voltage, conduction time, electrode distance, and emulsion species. A structural investigation of as-prepared polymer films allows us to propose two new structure build-up models. During a flat film deposition, isolated islands are formed first and grow on the substrate surface, and eventually, their mutual coalescence forms the final layer. Whereas, for a convex layer formation, the layer is first formed in the middle of the substrate and then grows toward the sides of the convex structure of the substrate. The results presented in this work expand the understanding of the mechanism of the DIFS process and may provide some new insights into structure-oriented multifunctional material design.

**Keywords** Polymer film; Emulsion; Demulsification-induced fast solidification; Mechanism

## 1 Introduction

Polymer films with well-defined composition and architecture are in growing demand due to their multi-functionalization and device integration[1—13]. Polymer films with varied compositions have been devoted to developing multitudinous materials. For example, polyurethane(PU) polymer films with varied module-like polymer structures show interesting and diverse properties, which are indispensable when it comes to excellent processability or maintaining good chemical durability[9—11]. In addition, rubber with satisfying chemical and physical properties, such as good resistance to chemicals, a large stretch ratio, and high resilience is used extensively in many applications, including aviation, healthcare, agriculture, national defense, and industry fields[12—14]. Polymer films are usually prepared by several methods, such as layer-by-layer assembly[15], casting[16], film-blowing[17], electropolymerization[18], and electrophoretic deposition (EPD)[19]. The environmental impact of these methods is a major concern in producing polymer films. Efforts toward environmentally friendly and safer polymer film production processes have led to the use of emulsion-based(*i.e.*, water-based) polymer films[20,21].

Emulsions formed by dispersing two immiscible liquids have been extensively studied in past years and exhibit a unique combination of physical and chemical properties due to their structure and composition adjustability[22,23]. These interesting emulsions are often used to prepare polymer films or coatings by casting and the EPD method[24—28]. It is difficult to manipulate the casting method to provide even polymer films or coatings in precise micrometer thickness due to the good fluidity of emulsion. At the same time, the EPD method possesses a higher deposition rate but usually needs high applied voltage(>40 V) since low voltage(<10 V) leads to slow deposition with a film thickness of only several micrometers[26—28]. Moreover, emulsions are thermodynamically unstable. Several processes may contribute to the emulsion breakdown, such as creaming, sedimentation, flocculation, phase inversion, coalescence, and Ostwald ripening[22,23]. Taking advantage of this property, a novel demulsification-induced fast solidification(DIFS) method was initially introduced by our group[29—32] to prepare functional polymer films overcoming the problems related to the earlier-mentioned deposition methods. In this process, an emulsion is demulsified *via* an electrochemical procedure based on its thermodynamic instability[30,32]. This approach allows micrometer control of the thickness of a large variety of

✉ ZHANG Jianfu
zhangjianfu@cust.edu.cn
✉ SU Zhongmin
zmsu@nenu.edu.cn
1. School of Materials Science and Engineering, Changchun University of Science and Technology, Changchun 130022, P. R. China;
2. School of Chemistry and Environmental Engineering, Changchun University of Science and Technology, Changchun 130022, P. R. China;
3. Jilin Provincial Science and Technology Innovation Center of Optical Materials and Chemistry, Changchun University of Science and Technology, Changchun 130022, P. R. China


https://doi.org/10.1007/s40242-022-1503-5

polymer films by adjusting the preparation parameters, *e.g.*, applied voltage($V$) and conduction time($t$)[30,32]. Moreover, the preparation process was fast, and the minimum time is only 10 s. In addition, to integrate different objects in these films, one can further engineer various film properties, for instance, by adjusting the crosslinking content, and incorporation of functional molecules of the emulsion, in which the polymer films are built or by adjusting other preparation parameters, such as electrode species, emulsion composition, and applied voltage[29—32]. Besides, this method demands less applied voltage with a minimum of only 0.5 V, enough to prepare uniform and thickness controllable film[30].

The DIFS method has been mainly applied to different types of emulsion systems till now[29—32]. However, a common rule to explain the build-up mechanism for almost all emulsion systems investigated is not established yet. Understanding how the polymer films are structured and what governs their solidification is extremely important for tuning their physicochemical properties. The existence of ions with a diffusion among the films was evident for the RE-906 polyurethane acrylate(906) system using metal alloy wires as anode and cathode[30]. However, the growth regime for common emulsions with different shapes of anode and cathode(sheet-wire, sheet-sheet, wire-wire) has not been shown directly for a given system. The present work investigates the build-up mechanism of polymer films obtained by the DIFS method by using waterborne polyurethane(WPU), polyvinyl acetate(PVAc), 906, and natural rubber(NR) emulsions. These emulsions were chosen because of their easy preparation, adjustable composition, excellent film forming ability, and environmental benignness[30,32].

Because of these unique physicochemical properties of the above emulsions, the resulting polymer films were expected to provide metal protective coatings with interesting metal bonding, functionalized polymer films, and so on.

Therefore, it was crucial to study the film structure for these systems. We first demonstrated the effect of electric field and ion diffusion collectively in the build-up process of polymer films. Secondly, the emulsion species were varied to validate the postulated build-up mechanism responsible for the electric field and ion diffusion growth regime, *i.e.*, the system growth dominated by the electric field and ion diffusion should thus be related to the conduction time, applied voltage, and emulsion parameters. This work presents the optimal preparation parameters, including conduction time, applied voltage, and the shape of electrode pairs for polymer film fabrication employing WPU, PVAc, 906, and NR emulsions to obtain the adjustable structure and surface morphology.

## 2 Experimental

### 2.1 Materials and Methods

Polyvinyl alcohol(PVA, 1799) was purchased from Anhui Wanwei Updated High-tech Material Industry Co., Ltd. (Chaohu, China). Dimethylolpropionic acid(DMPA), dibutyltin dilaurate(DBTDL), potassium peroxydisulfate(KPS), sodium dodecylsulfonate(SDS), vinyl acetate(VAc), and isophorone diisocyanate(IPDI) were purchased from Rhawn (Shanghai, China). Acetone was purchased from Tianjin Xintong Fine Chemicals Co., Ltd.(Tianjin, China). Triethylamine(TEA) was purchased from Beijing Chemical Works(Beijing, China). Sodium lauryl sulfonate(SLS) and octylphenol polyoxyethylene ether(OP-10) were purchased from Aladdin(Shanghai, China). Di-*n*-butyl phthalate(DBP) was purchased from Shenyang Xinhua Reagent Factory (Shenyang, China). Ethanol(EtOH, purity≥99.7%) and 1,4-butanediol(1,4-BD) were purchased from Sinopharm Chemical Reagent Co., Ltd.(Shanghai, China). The metal alloy wires(Al alloy, 750 μm diameter) were purchased from Changchun Metal Materials Corporation(Changchun, China). Zn sheets (100 μm) were purchased from Shanghai Xinqu Technology Co., Ltd.(Shanghai, China). Waterborne polycarbodiimide crosslinker(PCD, UN-557 type, solid content 40%) was purchased from Shanghai UN Chemical Co., Ltd.(Shanghai, China). 906 emulsion(solid content 52.0%±2.0%) was purchased from Bondly Chemical Co., Ltd.(Sihui, China). NR emulsion was purchased from Jinan Shiji Tiancheng Chemicals Co., Ltd.(Jinan, China). Poly-1,4-butylene adipate glycol(PBA, $M_w$=2000) was purchased from Qingdao Xinyutian Chemicals Co., Ltd.(Qingdao, China). Polycaprolactone(PCL, 2105, $M_w$=1000) was purchased from Hunan Juren Chemical New Mstar Technology Co., Ltd.(Yueyang, China). PBA and PCL were dried under vacuum for 2 h at 40 °C prior to use. All other materials were used as received without further treatment. Deionized water(DI) was used in all experiments.

### 2.2 Preparation of WPU Emulsion

Two WPU emulsions, WPU-A and WPU-L, were prepared according to previous work[32—34][Fig.1(A)]. A round bottom (1000 mL), three-necked separable flask with a mechanical stirrer and condenser was charged with PBA(36.65 g) or PCL(18.32 g), DMPA(1.55 g), and acetone. The mixture was stirred with an agitation speed of 300 r/min at 60 °C until a homogenous mixture was obtained. The catalyst DBTDL(400 μL) was added afterward, followed by adding IPDI(10.6 g) dropwise over 5 min, and the resulting mixture was stirred at


https://doi.org/10.1007/s40242-022-1503-5

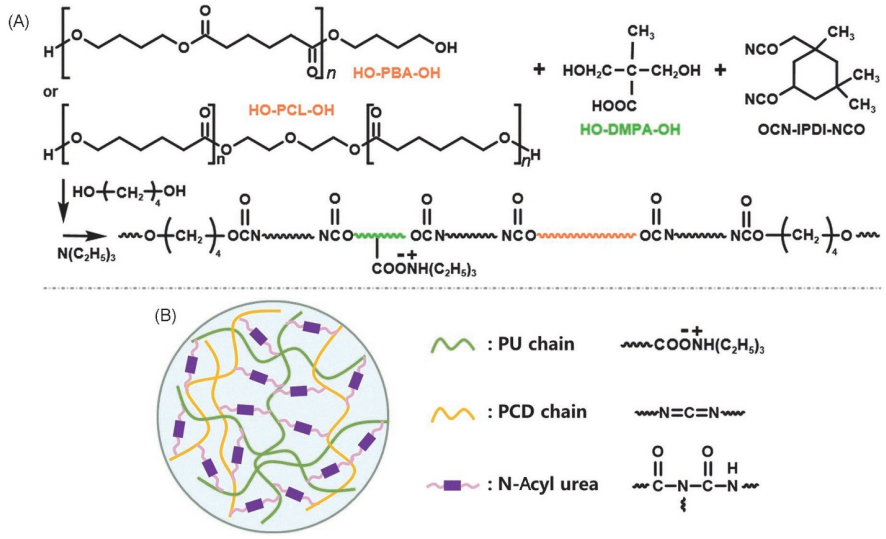


**Fig.1 Synthetic routes of WPU(A) and WPU/PCD(B) emulsions**

300 r/min for another 3 h at 60 °C. The prepolymer chain was extended by adding BD(2.144 g) and allowed to react for 2 h at 60 °C to obtain PU. Subsequently, the PU was neutralized by adding TEA(1.15 g) on stirring at 700 r/min for 30 min. Additional emulsifier, SLS(1.875 g), was then added and stirred at 1200 r/min for 30 min. Finally, the dispersion was obtained by slowly adding DI(79.614 g) to the above system, followed by stirring at a speed of 1400 r/min for 1 h at 50 °C. Finally, the acetone was removed at 50 °C on a rotary evaporator.

## 2.3 Preparation of WPU/PCD Emulsion

WPU/PCD emulsions, WPU-A/PCD-0.9 and WPU-L/PCD-1 (0.9 and 1 represent the PCD mass fractions to WPU-A/PCD-0.9 and WPU-L/PCD-1 emulsions, respectively) were prepared by adding PCD as a crosslinking agent to enhance the emulsion stability upon 400 r/min stirring for 1 h at 50 °C before rotary evaporation[Fig.1(B)][32].

## 2.4 Preparation of PVAc Emulsion

PVAc emulsion was prepared *via* radical polymerization[30]. PVA[120 mL, 1%(mass fraction) PVA in water] as a protective colloid and DI(48 mL) were added to a three-necked flask equipped with a mechanical agitator and a reflux condenser. The non-ionic emulsifier OP-10(3.2 mL), anionic emulsifier SDS(1 g), initiator KPS(10 mg/mL, 8 mL), and monomer VAc(20 mL) were added to the above reaction mixture and refluxed at 70 °C for 1 h with 350 r/min stirring. Then, VAc(108 mL) and KPS(10 mg/mL, 24 mL) were alternately added to the reaction as initiators, and the reaction was extended for 2 h. Afterward, the temperature was adjusted to 90 °C, and the reaction was continued for 1.5 h until no reflux was observed, followed by cooling to 50 °C. Finally, the plasticizer DBP(11.92 g) was added at 50 °C with stirring over 30 min.

## 2.5 Preparation of Polymer Films Based on the DIFS Method

The metal substrates were cleaned with EtOH followed by drying with airflow. Two cleaned metal substrates were used as electrodes with an appropriate parallel separation distance and immersed into an emulsion at room temperature. The WPU-A, WPU-L, WPU-A/PCD, WPU-L/PCD, PVAc, 906, and NR polymer films were fabricated on the surface of the anode by applying a direct current electric field for a certain time, followed by water rinsing to remove absorbed emulsion and drying at room temperature. For example, WPU(5 V, 20 min, 1 cm) indicates a polymer film fabricated on the Zn anode with an applied voltage of 5 V, 20 min conduction time, and a parallel separation distance of 1 cm. When metal alloy wires were used as both the anode and cathode, this preparation model was called the wire-wire(W-W) model. Using a Zn sheet as an anode and the metal alloy wire as cathode was designated a sheet-wire (S-W) model. In a sheet-sheet(S-S) model, both the anode and cathode were Zn sheets. The width of the Zn sheets immersed in the emulsion was 2.8 cm, and the anodes and cathodes immersed in the emulsion were of 1 cm height. The distance between electrodes was 1 cm. Free-standing polymer films were produced *via* mechanical exfoliation with a blade used for thickness measurement. The thickness of every free-standing film was calculated as the mean±standard deviation of at least five experimental determinations.


https://doi.org/10.1007/s40242-022-1503-5

### 2.6 Characterization

The viscosity of emulsions was determined *via* a rotary viscometer NDJ-5s(Shanghai FangRui Instrument Co., Ltd., Shanghai, China). Each viscosity represents the mean±standard deviation of at least three specimens. The thickness of the polymer films was measured with a micrometer caliper. The pH values of emulsions were obtained *via* pH test paper. The zeta potential and particle size of emulsions were obtained by a 90Plus particle size analyzer(Brookhaven, USA). The zeta potential and particle size of WPU-A and WPU-L emulsions were not shown due to their poor stability[32]. The morphology of the fabricated polymer films was obtained by a scanning electron microscope(SEM, XL-30 ESEM FEG, FEI/Phillips, Netherlands). The digital photo of the polymer films was obtained by a smartphone(Redmi K40 Pro+).

## 3 Results and Discussion

### 3.1 Preparation of Polymer Films *via* DIFS Method Based on the W-W Model

#### 3.1.1 Build-up Process of Polymer Films *via* DIFS Method Based on the W-W Model

Various emulsions, WPU-A, WPA-L, WPU-A/PCD, WPU-L/PCD, PVAc, 906, and NR emulsions, were utilized to investigate the build-up mechanism of the corresponding films prepared by the DIFS method. A stable emulsion is vital for a successful DIFS process, in which the emulsion has a suitable zeta potential(Table 1), which is not only conducive for demulsification but also ensures good emulsion stability. Other factors influencing the DIFS process includes applied voltage, conduction time, and emulsion parameters, such as emulsion viscosity, solid content, pH, particle size distribution, emulsion species, and film-forming ability of emulsion. Our previous study[30] has reported the build-up mechanism of 906 films with 1.0 V applied voltage and 1 cm electrode distance based on the W-W model[Fig.2(A)], *i.e.*, metal alloy wires were used as the anode and cathode. The film thickness was used to evaluate the polymer film build-up process. It was demonstrated that the build-up process of the 906 films strongly depended on ion diffusion and could be explained by Fick's second law[30]. However, significantly different behaviors were observed for WPU-A, WPA-L, WPU-A/PCD, WPU-L/PCD, PVAc, 906, and NR films when utilizing different voltages and emulsion species in the W-W model. Fig.2(B) shows the thickness of WPU-A/PCD films obtained in this study by varying the conduction time and applied voltage. The build-up process of WPU-A/PCD film(5 V, 1 cm) did not follow the Fick's second law well due to the lower determination coefficient($R^2$<0.9)[Fig.2(C)]. Consequently, two different growth regions were identified to describe the build-up process of the WPU-A/PCD films. In region I, the thickness of WPU-A/PCD films increases linearly with increasing the conduction time, identified *via* electric field process domination, which could be described *via* an EPD process[35—37], as shown in Fig.2(D). A linear function for the deposited thickness($h$) and time ($t$) can be expressed as:

$$h(t) = kt \quad (1)$$

This linear *h-t* kinetics is likely to remain over a certain time duration. During that time, the electric field dominates the emulsion particle deposition. However, when the conduction time increased over a critical value, the thickness of the WPU-A/PCD films showed a remarkable growth transition to weaker the conduction time-dependent linear kinetics, as depicted in Fig.2(E). This kinetic transition is probably resulted from ion diffusion becoming the main driving force of film growth due to the increased ion production with increasing conduction time according to the following reaction[30].

Anodic reaction:

$$\mathrm{Zn(s) + 2H_2O(l) - 6e^- \longrightarrow Zn^{2+} + O_2(g) + 4H^+} \quad (2)$$

Cathodic reaction:

$$\mathrm{H^+ + e^- \longrightarrow \frac{1}{2}H_2(g)} \quad (3)$$

The metal ions and $H^+$ produced on the surface of the anode induced demulsification of emulsions and fast solidification, initiating the film formation. After that, the ions diffused to the film surface, persisting the demulsification process and continuous film formation. The diffusion process of ions from the metal surface to the film surface is illustrated in Fig.2(F). There are several hypotheses of diffusion process[30]. (i) The

**Table 1 Parameters of WPU, WPU/PCD, PVAc, 906, and NR emulsions(the parameters of WPU, WPU/PCD emulsions are cited from ref.[32])**

| Emulsion | Solid mass fraction(%) | Viscosity/cp | pH value | Zeta potential/mV | Particle size /nm |
|---|---|---|---|---|---|
| WPU-A | 31.55±1.11 | 17.88±0.97 | 6.5 | —* | —* |
| WPU-L | 23.65±1.43 | 7.19±0.47 | 6.5 | —* | —* |
| WPU-A/PCD | 35.65±0.49 | 19.52±0.11 | 7.0 | −29.93±1.06 | 58.10±0.23 |
| WPU-L/PCD | 28.31±2.80 | 8.09±0.09 | 7.0 | −19.03±3.00 | 80.26±6.99 |
| PVAc | 36.13±0.77 | 16.27±0.06 | 2.7 | −12.67±0.51 | 326.05±3.61 |
| 906 | 51.87±0.40 | 589.64±3.11 | 5.5 | −28.07±0.70 | 282.95±3.04 |
| NR | 62.32±0.64 | 102.61±0.40 | 8.5 | −37.53±2.28 | 656.10±14.14 |

* Not being tested.


https://doi.org/10.1007/s40242-022-1503-5

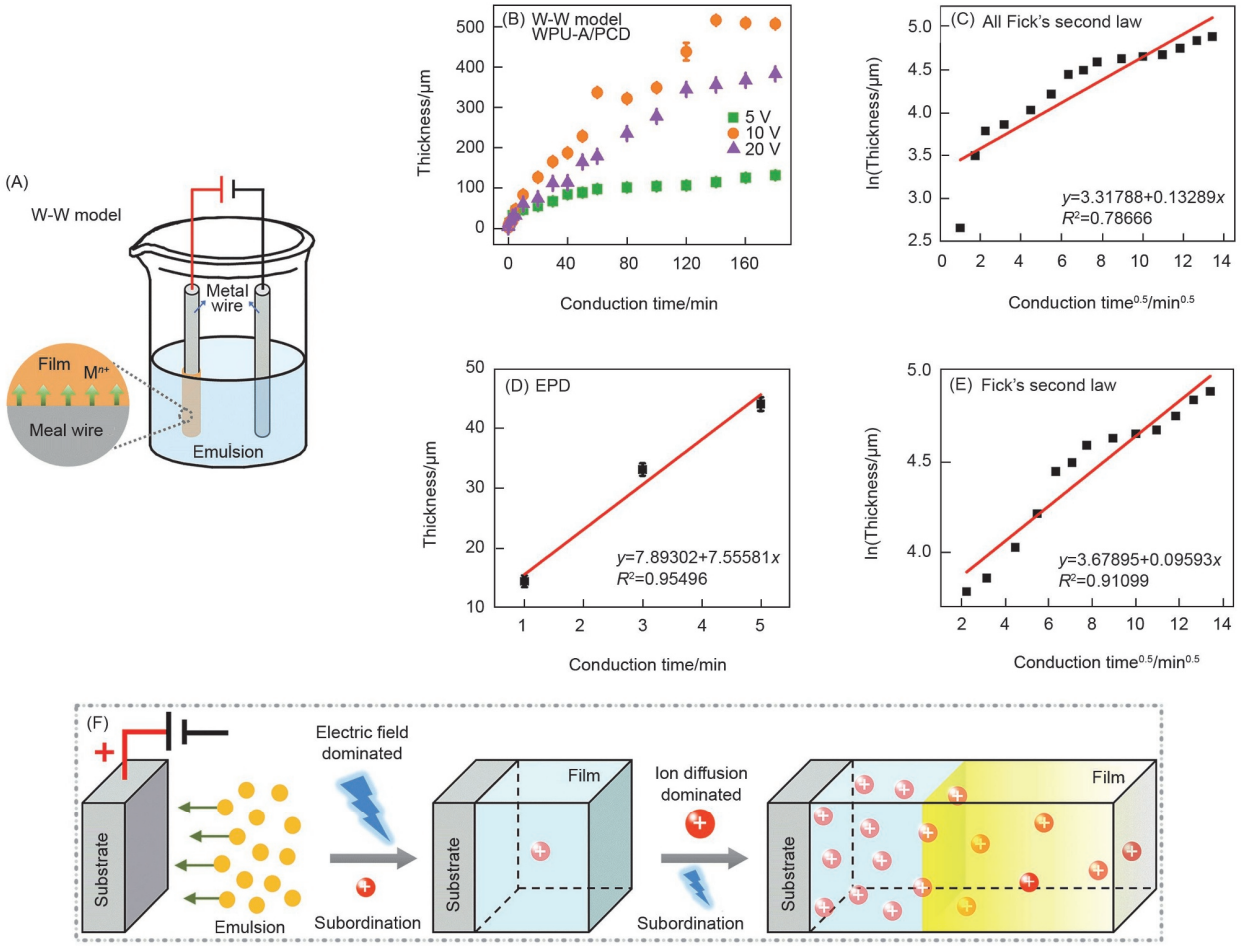


**Fig.2 Schematic diagram of the polymer film preparation process by the DIFS process in the W-W model(A), thickness of WPU-A/PCD films(5 V, 1 cm) as a function of the conduction time(the data of WPU-A/PCD films at applied voltage of 5 V were cited from ref.[32])(B), a square root of the time-natural logarithm of thickness from 1 min to 180 min for WPU-A/PCD film(5 V, 1 cm)(C), thickness of WPU-A/PCD film(5 V, 1 cm) plotted *versus* time for a short time from 1 min to 5 min of deposition(D), a square root of the time-natural logarithm of thickness approach for a long period from 5 min to 180 min of deposition of WPU-A/PCD film(5 V, 1 cm)(E) and schematic illustration of the process of the collective effect of the electric field and ion diffusion in the DIFS process**

solidification process takes place rapidly, immediately after demulsification, which occurs as soon as ions contact the emulsion; (ii) the film thickness is the ion transport rate, which can be described to the velocity from emulsion to solid; (iii) the ion content on the surface of the Zn substrate is constant, and there are no ions on the surface of the film(namely, the ion transport content decreased with the increase of the film thickness); (iv) the demulsification efficiency of each ion is equal; (v) the thicknesses of anode and cathode are enough to ensure sufficient ion production and ion transport required by the diffusion process; (vi) the film is homogeneous in three dimensions, so the ion diffusion is investigated in the vertical direction of the substrate[Fig.2(F)]. Thus, this process can be described *via* the Fick's second law of solution for a semi-infinite diffusion couple[30,38,39]. Especially when the concentration of ions $C(x,t)$ fit the following function:

$$c(x,t) = c_0 \operatorname{erfc}\frac{x}{2\sqrt{Dt}} \quad (4)$$

where $c_0$ is the initial ion concentration on the surface of the metal substrate, $D$ is the diffusion coefficient of ions generated by the electric field on the film surface, $t$ is the conduction time, and $x$ is the thickness of the film produced by ion diffusion. The diffusion distance $x$ is the distance from ion production to the film surface and can be expressed as:

$$x = D_f\sqrt{t} \quad (5)$$

The diffusion coefficients($D_f$) of the ions were calculated according to Eq.(6):

$$D_f = \frac{T}{\sqrt{t}} \quad (6)$$

where $T$ is the measured thickness. The relationship of the calculated diffusion coefficients $D_f$ and $t$ is shown in Fig.S1(A)(see the Electronic Supplementary Material of this paper), where $D_f$ decreases upon extending the conduction time. This observation collaborates with the assumption that the number of transmitted ions decreases when the film thickens. Hence, the polymer film thickness finally reached its maximum.


https://doi.org/10.1007/s40242-022-1503-5

The predictions from the ion diffusion fitted by the Fick's second law matched with our experiments[Fig.2(E)]. Notably, the build-up process was separately accompanied by an electric field and ion diffusion. However, the accompanying forces do not play a dominant role in the build-up process of films. Moreover, the time, at which time-dependent linear kinetics of the film growth transitions to a weaker time-dependent linear kinetics was dependent on the emulsion species. In order to exclude the influence of experimental errors and accidental factors on the film build-up process, we conducted three experiments on each kind of emulsion except for 906 and NR emulsions since they were purchased from the manufacturer in only one batch[WPU-A/PCD: Fig.S2 and Fig.S3, WPU-A: Figs.S4—S6, WPU-L: Figs.S7—S9, WPU-L/PCD: Figs.S10—S12, PVAc: Figs.S13—S15, 906: Fig.S16, and NR: Fig.S17(Fig.S2—Fig.S17 can be seen in the Electronic Supplementary Material of this paper). The variation in the one kind of film build-up processes might be explained by the differences in the emulsion batches caused by experimental errors and accidental factors.

Similar behavior was observed for WPU-A, WPU-L, WPU-L/PCD, and PVAc films in the W-W model(Fig.S4 and Fig.S15). Surprisingly, 906 and NR films showed a very different growth behavior, where the film thickness increased only for a short time(Fig.S16 and Fig.S17). After a while, the thickness became irregular, and it was impossible to get a good agreement with the EPD and Fick's second law process, which was attributed to the collective domination of electric field and ion diffusion resulting in an irregular deposition. The reason for the difference in the build-up process observed for the polymer films mentioned above could be attributed to the complexity of the different kinds of emulsion systems.

### 3.1.2 Effect of Applied Voltage and Conduction Time on the Formation of Polymer Films

The voltage applied during the DIFS process is a crucial parameter to be considered as it regulates the produced electric field, affecting the ion production, diffusion, and velocity of the particle deposition. Meanwhile, conduction time is also an essential parameter in the DIFS process, directly contributing to the amount of ion diffusion. The survey revealed that the deposition of the polymer films is dramatically influenced by the number of ions produced and their diffusion rate by controlling the applied voltage and conduction time[Fig.2(B) and Table 2]. Thus, by simply controlling the applied voltage and conduction time, it was possible to deposit thick and thin polymer films or, in some cases, completely prevent the polymer film deposition process. For example, when a voltage of 5 V was applied for the conduction time less than 10 s using the WPU-A/PCD emulsion, the film was difficult to be fabricated on anode due to insufficient ion production[Fig.2(B)]. During the construction of the WPU-A/PCD film, two types of structures were observed with increased conduction time. (i) A short conduction time(5 and 10 s, respectively) afforded island-type structures on the anodic surface[Fig.S1(B) and (C); (ii) a flat film could be observed when the conduction time increased(*e.g.*, 10 min), most probably due to the joining of islands forming a flat film[Fig.S1(D)]. In addition, applying a 0.5 V voltage[over than the standard electrode potential of $Fe^{2+}$ (–0.44 V)] or Zn-Cu galvanic cells to the WPU-A/PCD emulsions achieved the film fabrication on anode(Table 2). Noteworthy, the electrolysis of water occurs at more than 1.23 V. Furthermore, increasing the applied voltage beyond 10 V leads to porous and uneven film formation[Fig.S1(D)] because the emulsion becomes unstable at that voltage and the emulsion particles strongly agglomerate, further leading to uniform deposition. Besides, this porous structure can also be explained by huge amounts of gas produced at the anode[Eq.(3)] when applying high voltage for a longer time, making the film porous upon passing through it during the long deposition time. These results suggested that the structure of a DIFS film can be easily manipulated *via* the variation of applied voltage and conduction time. The fine-tuning of these parameters could be significant in the structural design of porous polymer films with more efficient

**Table 2 Films prepared by the W-W model**

| Sample | W-W model | Applied voltage/conduction time | Thickness/μm |
|---|---|---|---|
| WPU-A | Electrochemical cell | 1 V/82 h | 131.8±0.83666 |
| | | 1.5 V/70 h | 119.9±2.96648 |
| | | 2 V/14 h | 14.1±1.14018 |
| | | 2 V/96 h | 245.5±0.86603 |
| WPU-A/PCD | Electrochemical cell | 0.5 V/82 h | 86.2±0.83666 |
| | | 1.5 V/70 h | 519.2±1.03682 |
| | | 2 V/14 h | 217.9±3.69797 |
| | | 2 V/96 h | 451.8±15.91619 |
| WPU-A | Zn-Cu Galvanic cells | 14 h | 3±0.79057 |
| | | 12 d | 57.2±4.96991 |
| WPU-A/PCD | Zn-Cu Galvanic cells | 14 h | 11.4±1.14018 |
| | | 12 d | 156.4±4.94217 |


https://doi.org/10.1007/s40242-022-1503-5

permeability, physical adsorption, and drug loading, and the design of homogenous films for flexible and wearable materials.

### 3.2 Preparation of Polymer Films *via* DIFS Method Based on the S-W Model

Fig.3(A) shows the polymer film preparation process using the S-W model. A flat film can be fabricated by keeping the distance from 0.2 cm to 3 cm between the cathode and anode. The minimum electrode distance was kept more than 0.2 cm to reduce the experimental errors, and 1 cm distance was chosen as optimum to evaluate the growth process of the WPU-A/PCD film[Fig.3(B)]. First, the effect of varying the conduction time and applied voltage on the formation of WPU-A/PCD film on the surface of the Zn sheet was investigated. The effect of conduction time on the thickness of the WPU-A/PCD film at different voltages is displayed in Fig.3(C). Regardless of conduction time, increasing the applied voltage from 5.0 V to 20 V increased the thickness of the WPU-A/PCD film. At 5 V, the WPU-A/PCD film growth appears from "islands" to surface with varied time, as shown in Fig.3(D—I). Meanwhile, the gas evolution rate and the amount increased at voltages higher than 5.0 V, resulting in an irregular surface[Fig.3(J)] and bigger porous structure[Fig.3(K)] of the WPU-A/PCD film(20 V, 2 h, 1 cm). However, the thickness of the film does not change after reaching a maximum upon further increasing the voltage for a longer deposition time[Fig.3(C)], presumably due to the poor adhesion property of the film caused by the large amounts of

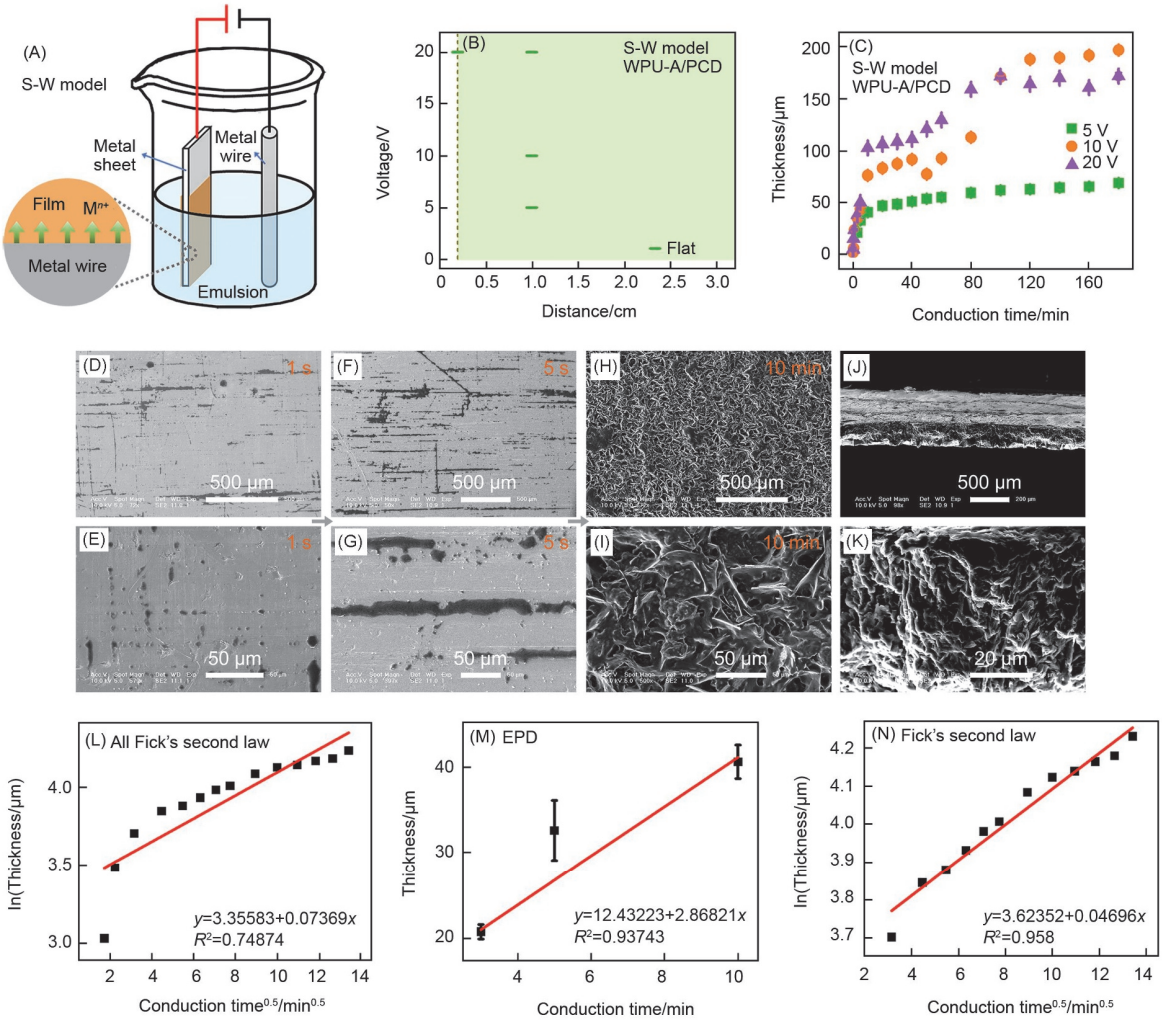


**Fig.3 Schematic diagram of film fabrication by the DIFS process in the S-W model(A), comparison of surface morphology by adjusting the voltage and distance between anode and cathode(B), thickness of WPU-A/PCD films with varied applied voltage as a function of the conduction time(the data of WPU-A/PCD films at applied voltage of 5 V are cited from ref.[32])(C), surface SEM image of the WPU-A/PCD film(5 V, 1 s, 1 cm)(D) and corresponding magnified image(E), SEM image of WPU-A/PCD film(5 V, 5 s, 1 cm)(F) and corresponding magnified images(G), SEM image of WPU-A/PCD film(5 V, 10 min, 1 cm)(H) and corresponding magnified image(I), SEM images of the cross-section of WPU-A/PCD film(20 V, 2 h, 1 cm)(J) and corresponding magnified image(K), a square root of the time-natural logarithm of thickness from 3 min to 180 min for WPU-A/PCD film(5 V, 1 cm)(L), thickness of WPU-A/PCD film(5 V, 1 cm) plotted *versus* time for a short time from 3 min to 10 min of deposition(M), and a square root of the time-natural logarithm of thickness approach for a long time from 10 min to 180 min of deposition of WPU-A/PCD film(5 V, 1 cm)(N)**


https://doi.org/10.1007/s40242-022-1503-5

gas evolved for longer deposition time. Another probable reason could be that the higher voltage produced more ions on the surface of the metal substrate, and the ions did not get enough time to diffuse in the film. Therefore, it could be concluded that the optimal applied voltage for fabricating the WPU-A/PCD film in the S-W model was 5 V as it is the highest voltage, at which a flat film surface and good adhesion can be formed. Meanwhile, the optimal conduction time was less than 80 min; increasing the conduction time further caused no improvement in the thickness of the film. Consequently, WPU-A/PCD films with maximum thickness, flat surface, and good adhesion were formed at low voltage and longer conduction time. Hence, the applied voltage of 5 V and electrode distance of 1 cm were chosen to observe the build-up mechanism of WPU-A/PCD film in the S-W model; the corresponding data are taken from our previous work[32][Fig.3(C)]. The build-up process did not adhere well to the Fick's second law[Fig.3(L)], which was also divided into two regimes. As shown in Fig.3(M) and (N), and Figs.S18—S20(see the Electronic Supplementary Material of this paper), the EPD process was exposed in the first stage, and ion diffusion fitted by the Fick's second law was used to describe the later stage. Similar growth behaviors were observed for WPU-A (Figs.S21—S23), WPU-L(Figs.S24—S26), WPU-L/PCD (Figs.S27—S29), PVAc(Figs.S30—S32), 906(Fig.S33), and NR films(Fig.S34). Fig.S21—Fig.S34 can be seen in the Electronic Supplementary Material of this paper.

Moreover, the film surface structure was also affected by emulsion species, but it was controllable by adjusting applied voltage and conduction time. For example, the morphology became completely different after the deposition PVAc, 906, and NR films. An exciting phenomenon was observed for the PVAc, 906, and NR films, where the films showed a convex surface with high deposition in the middle and low at both ends when the preparation parameters were in the red area[Fig.4(A) and (B)]. As evident from Fig.4(C) and (D), when the appliedvoltage was 5 V, electrode distance was 1 cm, and the conduction time was 1 and 5 s, the PVAc film could be formed only at the middle of the Zn sheet facing the cathode, and both sides were less. Next, the whole Zn sheet was coated with PVAc film by increasing the conduction time, as shown in Fig.4(E—G). Considering the distance, voltage, and conduction time dependence on the build-up process, it is clear that the structure evolved as a function of the distance, voltage, and conduction time. The convex surface was proportional to short time, high voltage, and

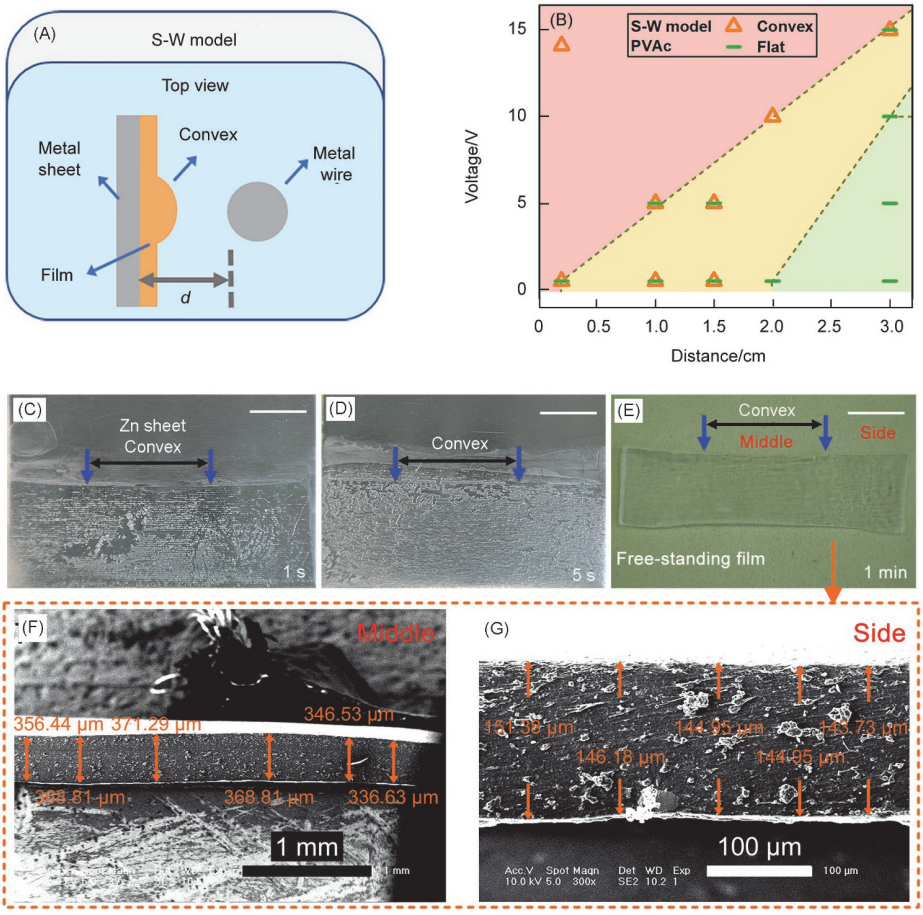


**Fig.4 Schematic illustration of the surface morphology of film with convex structure in the S-W model(*d* represents the parallel separation distance between anode and cathode)(A), comparison of surface morphology by adjusting the voltage and distance between anode and cathode(B), digital photos(scale bar: 5 mm) of surface of PVAc film(5 V, 1 s, 1 cm)(C), PVAc film(5 V, 5 s, 1 cm) (D), and PVAc film(5 V, 1 min, 1 cm)(E) and cross-section SEM images of PVAc film(5 V, 1 min, 1 cm) with middle(F) and side(G)**


https://doi.org/10.1007/s40242-022-1503-5

short distance. Such film formation occurs probably because the strong electric field originating in the middle of the electrode caused more deposition at the shortest distance, the middle part of the Zn sheet facing the electrode. As the distance and voltage were adjusted to 2 cm and 0.5 V, respectively, the convex surface of the PVAc film became inconspicuous for the entire period (0—180 min) and resulted in the formation of an almost flat film [Fig.S30(D—F)]. Thus, the parameters falling in the green area must be chosen to prepare a flat film, where the film growth from islet to surface[Fig.S30(D—F)] was the same as WPU-A/PCD film(5 V, 1 cm). During the build-up process of the PVAc films, a gradual structural patterning can be observed by adjusting the shape and size of the cathode in the red area, which was also observed for other groups(906: Fig.S33, and NR films: Fig.S34). Using the parameters of the yellow area, a flat or convex film could be prepared by adjusting the conduction time. Conclusively, electrode distance, applied voltage, and conduction time collectively played crucial roles during the DIFS process.

### 3.3 Preparation of Polymer Films *via* DIFS Method Based on the S-S Model

Fig.5(A) describes polymer film preparation by the S-S model. Fig.5(B) shows the evolution of the film thickness with the conduction time when the film was built at 5, 10, and 20 V, and electrode distance of 1 cm in the S-S model. The growth behavior of WPU-A/PCD films can be described in two regimes: the film growth was governed separately by the electric field and ion diffusion fitted by the Fick's second law[Fig.5(C—E) and Fig.S35, (see the Electronic Supplementary Material of this paper)]. The WPU-A/PCD films in the S-S model showed a surface morphology similar to the W-W and S-W models under the green area conditions, the transformation of islands[Fig.S35(B) and (C)] to a flat surface[Fig.S35(D)], where a relatively flat surface[Fig.S35(D)] with no convex in the middle was observed since the electric fields between electrodes were equal. The surface morphology was also affected by electrode distance, applied voltage, and conduction time. The effect of these parameters was even more noticeable on the films prepared with a long conduction time, higher voltage, and short electrode distance where the surface becomes quite irregular[Fig.S35(E)] for WPU-A/PCD film(20 V, 2 h, 0.5 cm). The irregular film surface may be resulted from the strongly agglomerated emulsion particles and evolution of a large amount of gas, causing an inhomogeneous deposition. Similarly, the growth behavior of WPU-L/PCD-repeated(Fig.S36 and Fig.S37), WPU-A(Figs.S38—S40), WPU-L(Figs.S41—S43), WPU-L/PCD (Figs.S44—S46), PVAc(Figs.S47—S49), 906(Fig.S50), and NR film (Fig.S51) was also studied by varying electric field and subsequent ion diffusion processes. Fig.S36—Fig.S51 can be seen in the Electronic Supplementary Material of this paper.

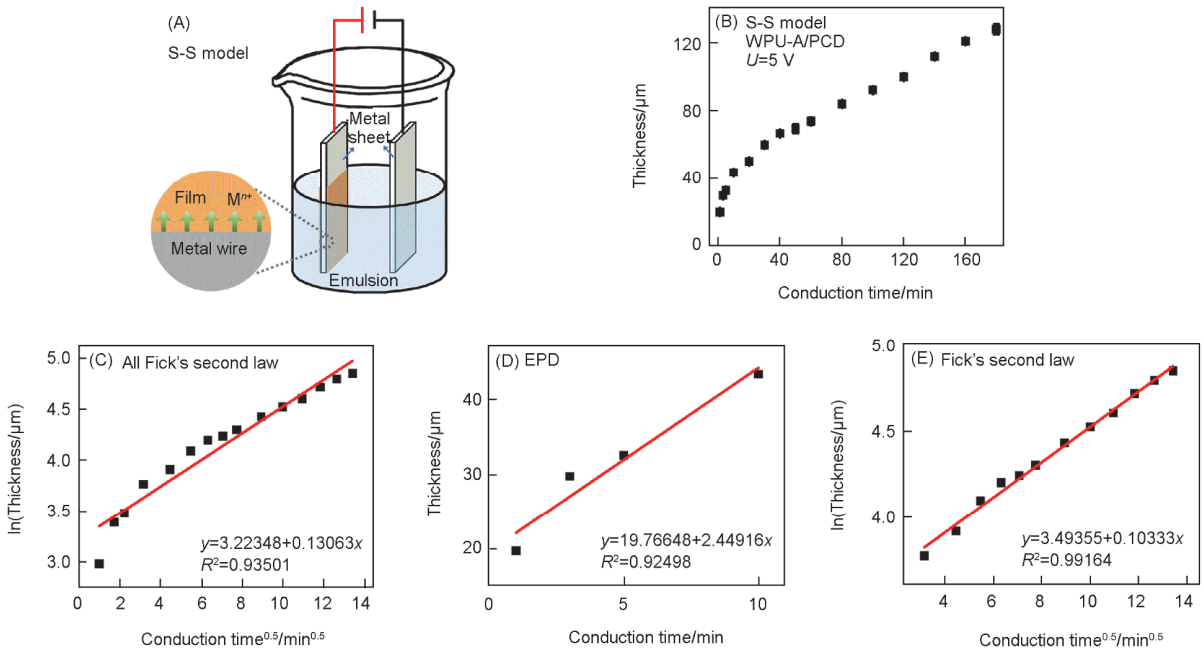


**Fig.5 Schematic diagram of film preparation by the DIFS process in the S-S model(A), thickness of WPU-A/PCD films(5 V, 1 cm) as a function of the conduction time(B), a square root of the time-natural logarithm of thickness from 1 min to 180 min for WPU-A/PCD film(5 V, 1 cm)(C), a thickness of WPU-A/PCD film(5 V, 1 cm) plotted *versus* time for a short time period from 1 min to 10 min of deposition(D), and a square root of the time-natural logarithm of thickness approach for a long time from 10 min to 180 min of deposition of WPU-A/PCD film(5 V, 1 cm)(E)**


https://doi.org/10.1007/s40242-022-1503-5

Based on all the above results, it is vital to emphasize that thickness analysis with curve fitting provided information about the growth process of the films prepared by the DIFS method, *i.e.*, film surface, and consequently, enabled the determination of the alternate preparation parameters, including applied voltage, conduction time, and electrode distance in order to adjust the film structure, which were applied for WPU-A, WPU-L, WPU-A/PCD, WPU-L/PCD, PVAc, 906, and NR films. Noteworthy, the above three kinds of electrode pair models in some respects are particular because, for all of them, the formation of polymer films can be affected by the applied voltage, conduction time, and electrode distance, and can form flat and porous structures within films. The formation of such porous structures can lead to film inhomogeneities at the micrometer length scale, favoring the electric field and ion diffusion. Moreover, during the polymer film growth process by the above three kinds of electrode pair models, ion diffusion plays the leading role, whereas electric field and ion diffusion separately present their role in the early and later stages or the theses two factors collectively played a dominated role, which are related to the formation factors of polymer film, including voltage and emulsion parameters. Interestingly, the electric field has a greater effect on PVAc, 906, and NR emulsions than WPU and WPU/PCD emulsions, which was proved from the S-W model, showing the convex structure of PVAc, 906, and NR films resulted from the strong electric field originating by the short distance. The result was different for WPU and WPU/PCD films, which were flat in all electrode distances ranging from 0.2 cm to 3 cm. The data extracted from Figs.S13, Fig.S30, and Fig.S47 for PVAc, Fig.S16, Fig.S33, and Fig.S50 for 906, and Fig.S17, Fig.S34, and Fig.S51 for NR films shown in Fig.S52(see the Electronic Supplementary Material of this paper) further confirm this explanation. The electric field was enhanced in the S-S model compared to the W-W model, which distinctively increased the thickness of the PVAc, 906, and NR films, but no significant increment in the thickness for WPU and WPU/PCD films in three kinds of electrode models was observed.

## 4 Conclusions

This work demonstrated the build-up process and micro-scale structure adjustment of polymer films prepared by the DIFS method. Collectively electric field and ion diffusion were proved to govern the film build-up process. Especially, the thickness and structure of the prepared films showed high dependency on the applied voltage, conduction time, electrode distance, and emulsion species. The film thickness could be tuned by concomitantly controlling the electric field and ion diffusion process. Furthermore, the structural investigation of the prepared films opens new scenarios in films build-up mechanisms that are contributed by both electric field and ion diffusion interactions. The varied electric field steered the formation of the convex and flat surface structure of the polymer films in the S-W model and was identified as the major factor regulating the polymer film formation in this study. Further, porous and homogeneous polymer film structures could also be formed by adjusting the preparation parameters. Therefore, this study presents substantial progress in the elucidation and understanding of the polymer film build-up mechanism and the structure of films, which is essential for micro-scale film design and sheds new light on controlling the multifunctional film materials.

### Electronic Supplementary Material

Supplementary material is available in the online version of this article at http://dx.doi.org/10.1007/s40242-022-1503-5.

### Acknowledgements

This work was supported by the Science and Technology Development Planning Project of Jilin Province, China(No.20200401037GX) and the National Natural Science Foundation of China(No.21504008).

### Conflicts of Interest

The authors declare no conflicts of interest.

## References

[1] Yoo J. J., Seo G., Chua M. R., Park T. G., Lu Y. L., Rotermund F., Kim Y.-K., Moon C. S., Jeon N. J., Correa-Baena J.-P., Bulović V., Shin S. S., Bawendi M. G., Seo J., *Nature*, **2021**, *590*, 587
[2] Yang F., Li J., Long Y., Zhang Z. Y., Wang L. F., Sui J. J., Dong Y. T., Wang Y. Z., Taylor R., Ni D. L., Cai W. B., Wang P., Hacker T., Wang X. D., *Science*, **2021**, *373*, 337
[3] Mahato A. K., Bag S., Sasmal H. S., Dey K., Giri I., Linares-Moreau M., Carbonell C., Falcaro P., Gowd E. B., Vijayaraghavan R. K., Banerjee R., *J. Am. Chem. Soc.*, **2021**, *143*, 20916
[4] Chen L. J., Hao C. L., Cai J. R., Chen C., Ma W., Xu C.L., Xu L. G., Kuang H., *Angew. Chem. Int. Ed.*, **2021**, *60*, 26276
[5] Zheng S. J., Li W. Z., Ren Y. Y., Liu Z. Y., Zou X. Y., Hu Y., Guo J. N., Sun Z., Yan F., *Adv. Mater.*, **2021**, 2106570
[6] Ren W., Lin G. G., Clarke C., Zhou J. J., Jin D.Y., *Adv. Mater.*, **2019**, 32, 1901430
[7] Wang Z., Jiang X. Y., Huang K., Ning L., Zhang J. Q., Zhang F. L., Yang J. G., Wu Y. C., Chen X. D., Yi Y. P., Shi X. H., Chen Y., Wang S. T., *Adv. Mater.*, **2021**, 2106067
[8] Liu J. P., Zhang P., Wei H. Q., Lu Z., Yu Y., *Adv. Funct. Mater.*, **2021**, 2107732
[9] de Luna M. S., Wang Y., Zhai T., Verdolotti L., Buonocore G. G., Lavorgna M., Xia H., *Prog. Polym. Sci.*, **2019**, *89*, 213
[10] Lu J. Y., Zhang Y., Tao Y. J., Wang B. B., Cheng W. H., Jie G. X., Song L., Hu Y., *J. Colloid Interface Sci.*, **2021**, *588*, 164
[11] Lee J. I., Choi H., Kong S. H., Park S., Park D., Kim J. S., Kwon S. H., Kim J., Choi S. H., Lee S. G., Kim D. H., Kang M. S., *Adv. Mater.*, **2021**, *33*, 2100321
[12] Ahmadi Y., Ahmad S., *Polym. Rev.*, **2020**, *60*, 226
[13] Gao H. Y., Liu H. J., Song C. Z., Hu G. X., *Chem. Eng. J.*, **2021**, *368*, 1013
[14] Cao L.M., Cheng Z. Z., Yan M. W., Chen Y. K., *Chem. Eng. J.*, **2019**, *363*, 203
[15] Zhang X. L., Xu Y., Zhang X., Wu H., Shen J. B., Chen R., Xiong Y., Li J., Guo S. Y., *Prog. Polym. Sci.*, **2019**, *89*, 76
[16] Yu L. Y., Pavlica E., Li R. P., Zhong Y. F., Silva C., Bratina G., Müller C., Amassian A., Stingelin N., *Adv. Mater.*, **2021**, 2103002
[17] Zhang Q. L., Chen W., Zhao H. Y., Ji Y. X., Meng L. P., Wang D. L., Li L. B., *Polymer*, **2020**, *198*, 122492
[18] Yang M., Yang T. T., Deng H. J., Wang J. J., Ning S., Li X., Ren X. N., Su Y. M., Zang J. F., Li X. J., Luo Z. Q., *Adv. Funct. Mater.*, **2021**, *31*, 2105857
[19] Deen I., Selopal G. S., Wang Z. M., Rosei F., *J. Colloid Interface Sci.*, **2022**, *607*, 869
[20] Dastjerdi Z., Cranston E. D., Berry R., Fraschini C., Dubé M. A., *Macromol. React. Eng.*, **2019**, *13*, 1800050

[21] Zhang Y., Dubé M. A.; Eds. Pauer W., *Green Emulsion Polymerization Technology, in Advances in Polymer Science: Polymer Reaction Engineering of Dispersed Systems*, (Eds: Pauer W.,), Springer, Berlin, Heidelberg, **2017**, *280*, 1
[22] Chern C. S., *Prog. Polym. Sci.*, **2006**, *31*, 443
[23] Wang Q., Fu S. K., Yu T. Y., *Prog. Polym. Sci.*, **1994**, *19*, 703
[24] Cui P. C., Wu S. L., Xie J., Ma J. Y., Ding L. Y., Olasoju O. S., Cao Y. J., Li Y. Q., Shen L. Y., Sun W., *Chem. Commun.*, **2021**, *57*, 6620
[25] Li M., Liu W. F., Zhang Q., Zhu S. P., *ACS Appl. Mater. Interfaces*, **2017**, *9*, 15156
[26] Jugowiec D., Łukaszczyk A., Cieniek Ł., Kowalski K., Rumian Ł., Pietryga K., Kot M., Pamuła E., Moskalewicz T., *Surf. Coat. Technol.*, **2017**, *324*, 64
[27] Zhang J., Dai C. S., Wei J., Wen Z. H., *Appl. Surf. Sci.*, **2012**, *261*, 276
[28] Kim S., Oh J.-S., Hwang T., Cho M., Lee Y., Choi H.R., Kim S. W., Nam J.-D., *Korea Aust. Rheol.*, **2013**, *25*, 261
[29] Wang D., Kong R. X., Ge X. S., Yao Z. H., Zhou Y., Zhang J. F., *Macromol. Mater. Eng.*, **2019**, *304*, 1900250
[30] Wang D., Ge X. S., Nie H. R., Yao Z. H., Zhang J. F., *Chem. Commun.*, **2019**, *55*, 9192
[31] Wang D., Ge X. S., Zhang J. F., Su Z.M., *Chem. Res. Chinese Universities*, **2019**, *35*(6), 1082
[32] Wang D., Li J. Y., Wang Y. K., Omoniyi A. O., Fu Z. W., Zhang J. F., Su Z.M., *Chem. Eng. J.*, **2021**, 134055
[33] Nanda A. K., Wicks D. A., *Polymer*, **2006**, *47*, 1805
[34] Madbouly S. A., Otaigbe J. U., *Prog. Polym. Sci.*, **2009**, *34*, 1283
[35] Sarkar P., Nicholson P. S., *J. Am. Cernm. Soc.*, **1996**, *79*, 1987
[36] Chen C.-Y., Chen S.-Y., Chen D.-M., *Acta Mater.*, **1999**, *47*, 2717
[37] Wang Y. C., Leu I.-C., Hon M.-H., *J. Am. Cernm. Soc.*, **2004**, *87*, 84
[38] Paul A., Laurila T., Vuorinen V., Divinski S. V., *Thermodynamics, Diffusion and the Kirkendall Effect in Solids*, Springer, Cham Heidelberg, New York, Dordrecht, London, **2014**
[39] Shlosman K., Suckeveriene R. Y., Rosen-Kligvasser J., Tchoudakov R., Zelikman E., Semiat R., Narkis M., *Polym. Adv. Technol.*, **2014**, *25*, 1484